Adaptive analog nonlinear circuits for improving properties of electronic devices

Out-of-band and adjacent-channel interference reduction by analog nonlinear filters

In a perfect-world communication technology we would have “brick wall" filters, no-distortion amplifiers and mixers, and well-coordinated spectrum operations. The real world, however, is prone to various types of unintentional and intentional interference of technogenic (man-made) origin that can disrupt critical defense communication systems, with the impacts ranging from slight reduction in the channel capacity to the channel failure. In this paper, we introduce a methodology for mitigation of technogenic interference in communication channels by analog nonlinear filters, with a particular emphasis on the mitigation of the out-of-band and the adjacent-channel interference.

Interference induced in a communications receiver by external transmitters can be viewed as a wide-band non-Gaussian noise affecting a narrower-band baseband signal of interest. In many cases this noise may contain a strong component within the passband of the receiver, which may dominate over the thermal noise. While the total wide-band interference seen by the receiver may or may not be impulsive (e.g. characterized by a high degree of peakedness), we demonstrate that the interfering component due to power emitted by the transmitter into the receiver channel is likely to appear impulsive under a wide range of conditions, especially if observed at a sufficiently wide bandwidth. When a linear filter is used to suppress the interference outside of the passband of interest, the resulting signal quality is invariant to the type of the amplitude distribution of the interfering signal, as long as the total power and the spectral composition of the interference remain unchanged. However, the spectral density of a non-Gaussian interference in the signal passband can be reduced, without significantly affecting the signal of interest, by introducing an appropriately chosen feedback-based nonlinearity into the response of the linear filter.

In particular, impulsive interference characterized by frequent occurrence of outliers can be effectively mitigated by the Nonlinear Differential Limiter (NDL) described in this paper. An NDL can be configured to behave linearly when the input signal does not contain outliers, but when the outliers are encountered, the nonlinear response of the NDL limits the magnitude of the respective outliers in the output signal. As a result, the signal quality is improved in excess of that achievable by the respective linear filter, increasing the capacity of a communications channel. The behavior of an NDL and its degree of non-linearity is controlled by a single parameter in a manner that enables significantly better overall suppression of the noise containing impulsive components compared to the respective linear filter. Adaptive configurations of NDLs are similarly controlled by a single parameter, and are suitable for improving quality of non-stationary signals under time-varying noise conditions. NDLs are designed to be fully compatible with existing linear devices and systems, and to be used as an enhancement, or as a low-cost alternative, to the state-of-art interference mitigation methods.

We demonstrate that the most effective way to suppress out-of-band and adjacent-channel interference is to deploy an appropriately chosen linear filter in the signal chain of the receiver preceding an NDL. This filter can selectively suppress the non-impulsive component of the total interference without affecting the baseband signal of interest, while increasing the peakedness of the remaining interference affecting the baseband signal, thus increasing the effectiveness of interference mitigation by a subsequently deployed NDL.

1 Introduction and motivation

In a utopian world, our communication technology would have "brick wall" filters, no-distortion amplifiers and mixers, and well-coordinated spectrum operations. In the real world, wireless communications are prone to various types of natural and technogenic (man-made) interference. Over the years engineers developed effective filters and approaches to dealing with natural interference, but the need to transmit more and more data leads to ever-increasing levels of technogenic interference as we saturate the information carrying capacity of the electromagnetic spectrum. This brings the understanding of the types of technogenic interference and development of effective ways of its mitigation to the forefront of challenges facing modern communication technology.

Technogenic noise comes in a great variety of forms, but it will typically have a temporal and/or amplitude structure which distinguishes it form the natural (e.g. thermal) noise. It will typically also have non-Gaussian amplitude distribution. These features of technogenic noise provide an opportunity for its mitigation by nonlinear filters, especially for the in-band noise, where linear filters that are typically deployed in the communication receiver (see top part of figure 1) have very little or no effect. Indeed, at any given frequency, a linear filter affects both the noise and the signal of interest proportionally. When a linear filter is used to suppress the interference outside of the passband of interest, the resulting signal quality is affected by the total power and spectral composition, but not by the type of the amplitude distribution of the interfering signal. On the other hand, the spectral density of a non-Gaussian interference in the signal passband can be reduced, without significantly affecting the signal of interest, by introducing an appropriately chosen feedback-based nonlinearity into the response of the linear filter.

In particular, impulsive interference that is characterized by frequent occurrence of outliers can be effectively mitigated by the Nonlinear Differential Limiters (NDLs) described in [9, 8, 11] and in Section 3 of this paper. An NDL can be configured to behave linearly when the input signal does not contain outliers, but when the outliers are encountered, the nonlinear response of the NDL limits the magnitude of the respective outliers in the output signal. As a result, the signal quality is improved in excess of that achievable by the respective linear filter, increasing the capacity of a communications channel. Even if the interference appears non-impulsive, the non-Gaussian nature of its amplitude distribution enables simple analog pre-processing which can increase its peakedness and thus increase the effectiveness of the NDL migitation.

Another important consideration is the dynamic non-stationary nature of technogenic noise. When the frequency bands, modulation/communication protocol schemes, power levels, and other parameters of the transmitter and the receiver are stationary and well defined, the interference scenarios may be analyzed in great detail. Then the system may be carefully engineered (albeit at a cost) to minimize the interference.[1] It is far more challenging to quantify and address the multitude of complicated interference scenarios in non-stationary communication systems such as, for example, software-defined radio (SDR)-based and cognitive *ad hoc* networks comprising mobile transmitters and receivers, each acting as a local router communicating with a mobile *ad hoc* network (MANET) access point. In this scenario, the transmitter positions, powers, and/or spectrum allocations may vary dynamically. In multiple access schemes, the interference is affected by the varying distribution and arrangement of transmitting nodes. In addition, with MANETs, the fading distribution also varies dynamically, and the path loss distribution is unbounded. With spectrum-aware MANETs, frequency allocations could also depend on various criteria, e.g. whitespace and the customer quality of service goals. This is a very challenging situation which requires the interference mitigation tools to adapt to the dynamically changing interference. Following the dynamic nature of the *ad hoc* networks, where the networks themselves are scalable and adaptive, and include spectrum sensing and dynamic re-configuration of the network parameters, the interference mitigation tools are needed to be scalable and adaptive to the dynamically changing interference. The Adaptive NDLs (ANDLs) [8, 11] have been developed to address this challenge.

Based on the above considerations, we propose a modification of a communications receiver system as illustrated in the bottom part of figure 1, where an NDL or ANDL filter is used as a replacement, or in conjunction with the existing mixer/linear filters.

To give more specificity to our presentation, let us consider a single transmitter-receiver system. Figure 2 provides a simplified qualitative illustration of different contributions into the interference which a receiver (RX) experiences from a transmitter (TX). Since real time “brick-wall" filters are not physically realizable as they have infinite latency (i.e. their compact support in the frequency domain forces their time responses not to have compact support, meaning that they are ever-lasting) and infinite order (i.e. their responses cannot be expressed as a linear differential equation with a finite sum), TX emissions would “leak" outside of the nominal (allocated) passband of a TX channel $[f_1, f_2]$ as out-of-band (OOB) emissions. Likewise, an RX filter would have non-zero response outside of its nominal (allocated) passband $[f_3, f_4]$. As a result, there is non-zero interference from the TX into the RX.

The total power of this interference may be broken into three parts. Part I is the power of the TX signal in its nominal band $[f_1, f_2]$, weighted by the response of the RX filter in this band. Part II is the TX OOB emissions in the RX nominal band $[f_3, f_4]$, weighted by the response of the RX filter in this band. The rest of the interference power comes from the TX emissions outside of the nominal bands of both channels, and can be normally ignored in practice since in those frequency regions both the emitted TX power and the RX filter response would be relatively small.

[1] For example, the out-of-band (OOB) emissions of a transmitter may be greatly reduced by employing a high quality bandpass filter in the antenna circuit of the transmitter. Such an additional filter, however, may negatively affect other properties of a system, for example, by increasing its cost and power consumption (due to the insertion loss of the filter).

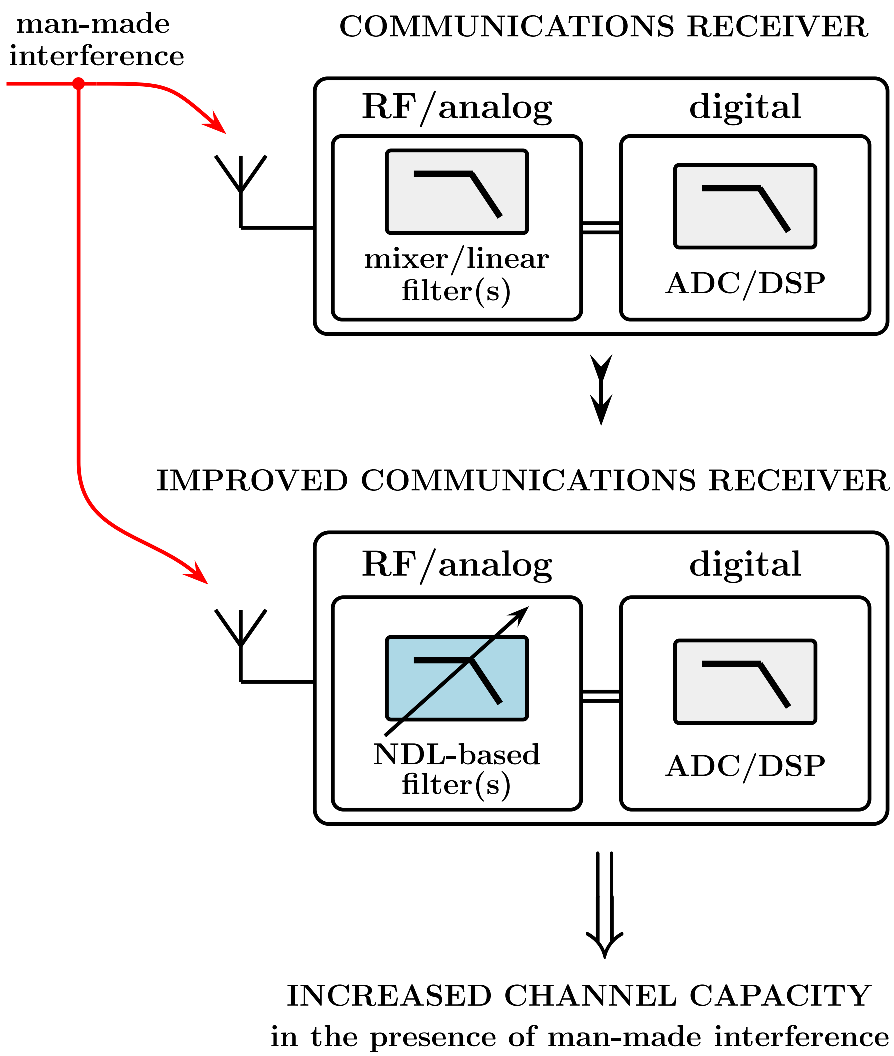

Figure 1: Simplified diagram of improving receiver performance in the presence of technogenic (man-made) interference.

While part I of the interference contributes into the total power in the RX channel and may cause RX overload, it does not normally degrade the quality of the communications in the RX since the frequency content of this part of the interference lies outside of the RX channel. Part II, however, in addition to contributing to overload, also causes degradation in the RX communication signal as it raises the noise floor in the RX channel.

Theoretical [6, 7] as well as the experimental [10] data suggest that the TX OOB interference in the RX channel (part II of the interference in figure 2) can appear impulsive under a wide range of conditions, as will be additionally illustrated in Section 2. While this interference cannot be reduced by the subsequent linear filtering in the RX channel, it may be effectively mitigated by such nonlinear filters as the NDLs.

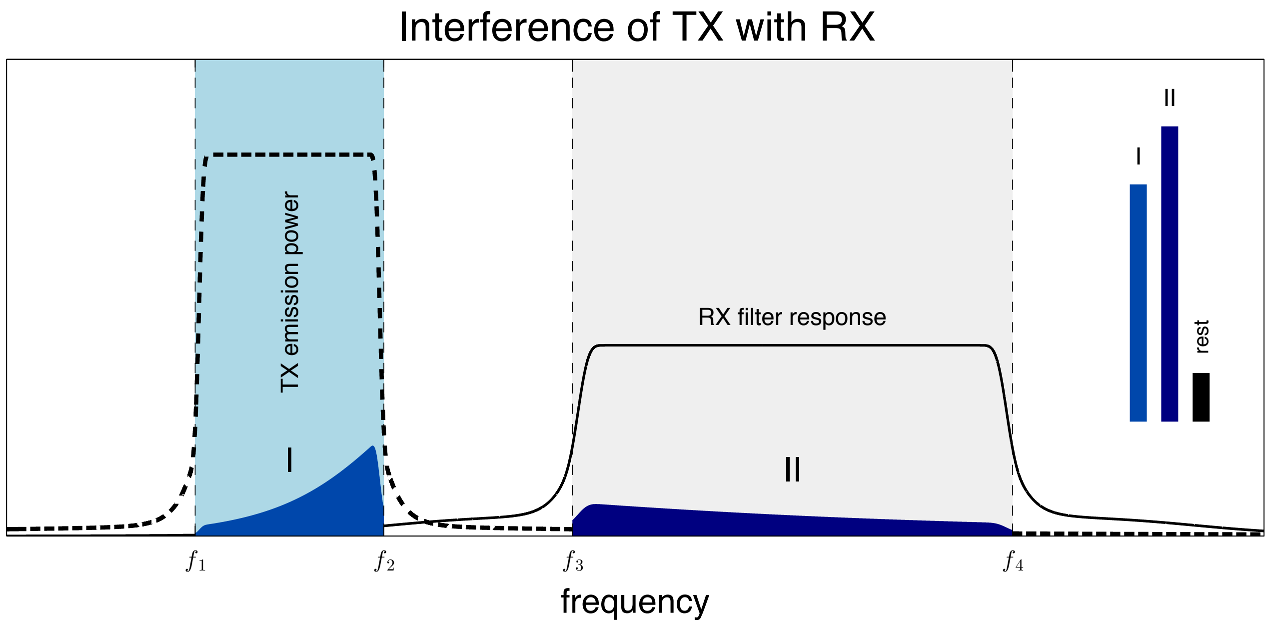

Figure 2: Qualitative illustration of different contributions into the interference which a receiver (RX) experiences from a transmitter (TX).

In Section 4 we show that an NDL deployed in the RX channel can reduce the spectral density of impulsive interference in the signal passband without significantly affecting the signal of interest, thus improving the baseband signal-to-noise ratio and increasing the channel capacity. We also show that, when part I of the interference in figure 2 dominates over part II and the total interference observed in the receiver does not appear impulsive, one can deploy a bandstop linear filter in the signal chain of the receiver preceding the NDL to suppress part I of the interference without affecting the baseband signal of interest. By suppressing part I of the interference and thus increasing the peakedness of the remaining interference affecting the baseband signal, this additional filter can greatly improve the effectiveness of interference mitigation by the subsequently deployed NDL. In Section 5 we provide some concluding remarks, and comment on the possibility of digital implementations and deployment of the NDLs.

2 Impulsive nature of interchannel interference

As shown in more detail in [6, 7], with additional experimental evidence presented in [10], the signal components induced in a receiver by out-of-band communication transmitters can appear impulsive under a wide range of conditions. For example, in the transmitter-receiver pair schematically shown at the top of figure 3, for a sufficiently large absolute value of the difference between the transmit and receive frequencies $\Delta f = f_{\mathrm{RX}} - f_{\mathrm{TX}}$, the instantaneous power $I^2(t, \Delta f) + Q^2(t, \Delta f)$ of the in-phase and quadrature components of the receiver signal may appear as a pulse train consisting of a linear combination of pulses originating at discrete times and shaped as the squared impulse response of the receiver lowpass filter.

For a single transmitter, the typical intervals between those discrete times are multiples of the symbol duration of the transmitted signal (or other discrete time intervals used in the designed modulation scheme, for example, chip and guard intervals). The non-idealities in hardware implementation of designed modulation schemes such as the non-smooth behavior of the modulator around zero, and/or nonlinearities in the power amplifier, can also lead to appearance of additional discrete origins for the pulses and exacerbate the OOB emissions. If the typical value of those discrete time intervals is large in comparison with the inverse bandwidth of the lowpass filter in the receiver, this pulse train may be highly impulsive.

A key mathematical argument leading to this conclusion can be briefly recited as follows. The total emission from various digital transmitters can be written as a linear combination of the terms of the following form:

$$x(t) = A_T(\bar{t})\, \mathrm{e}^{\mathrm{i}\omega_\mathrm{c} t}\,, \tag{1}$$

where ω_c is the frequency of a carrier, $\bar{t} = \frac{2\pi}{T}\, t$ is *nondimensionalized time*, and $A_T(\bar{t})$ is the desired (or designed) complex-valued modulating signal representing a data signal with symbol duration (unit interval) T. Let us assume that the impulse response of the lowpass filters in both channels of a quadrature receiver is $w(t) = \frac{2\pi}{T}\, h(\bar{t})$, and that the order of the filter is larger than n so that all derivatives of $w(t)$ of order smaller or equal to $n-1$ are continuous.[2] Let us now assume that all derivatives of the same order of the modulating signal $A_T(\bar{t})$ are finite, but the derivative of order $n-1$ of $A_T(\bar{t})$ has a countable number of step discontinuities[3] at $\{\bar{t}_i\}$. Then, if $\Delta\omega = 2\pi\Delta f$ is the difference between the receiver and the carrier frequencies, and the bandwidth of the lowpass filter $w(t)$ in the receiver is much smaller than $|\Delta f|$, the instantaneous power in the quadrature receiver due to $x(t)$ can be expressed as[4]

$$\begin{aligned} P_x(t,\Delta f) \;&=\; \frac{1}{(T\,\Delta f)^{2n}} \sum_i \alpha_i\, h\left(\bar{t}-\bar{t}_i\right) \sum_j \alpha_j^*\, h\left(\bar{t}-\bar{t}_j\right) \\ &\quad \text{for} \quad T\Delta f \gg 1\,, \end{aligned} \tag{2}$$

where α_i is the value of the ith discontinuity of the order $n-1$ derivative of $A_T(\bar{t})$,

$$\alpha_i = \lim_{\varepsilon\to 0} \left[A_T^{(n-1)}(\bar{t}_i+\varepsilon) - A_T^{(n-1)}(\bar{t}_i-\varepsilon) \right] \neq 0\,. \tag{3}$$

When viewed as a function of both time and frequency, the interpretation of (2) for the instantaneous power in a quadrature receiver is a *spectrogram* [see 3, for example] in the time window $w(t)$ of the term $x(t)$ of the transmitted signal. Figure 3 provides an illustrative example of such spectrograms for the $I^2(t,\Delta f) + Q^2(t,\Delta f)$ receiver signal in the transmitter-receiver pair schematically shown at the top of the figure.

[2] In general, if n is the order of a causal analog filter, then $n-1$ is the order of the first discontinuous derivative of its impulse response.

[3] One will encounter discontinuities in a derivative of some order in the modulating signal sooner or later, since any physical pulse shaping is implemented using causal filters of finite order.

[4] Equation (2) will still accurately represent the instantaneous power in the quadrature receiver if the "real" (physical) modulating signal can be expressed as $A(t) = \psi(t) * A_T(t)$, where the convolution kernel $\psi(t)$ is a lowpass filter of bandwidth much larger than $|\Delta f|$.

The spectrograms displayed in the panels of the figure show the instantaneous power response of a quadrature receiver tuned to the RX frequency f_{RX}, where f_{RX} is in the 1 GHz to 3 GHz range. The transmitted signal is in a 5 MHz band around 2 GHz, the transmit power is 125 mW (21 dBm), and the path/coupling loss is 50 dB. A more detailed description of the simulation parameters used in figure 3 and the subsequent examples can be found in Appendix A.

In panels I(a) and I(b) of figure 3, the bandwidth of the lowpass filter (8th order Butterworth) is 40 MHz (wide), while in panels II(a) and II(b) it is 5 MHz (narrow). Panels I(a) and II(a) show the receiver power due to the transmitter signal only (without thermal noise), while panels I(b) and II(b) show the receiver power with additive white Gaussian noise (AWGN) taken as the thermal noise multiplied by the noise figure of the receiver (assumed 5 dB). The shape of the impulse response (time window) $w(t) = \frac{2\pi}{T}\, h(\bar{t})$ of the lowpass filters is shown in the upper left corners of the respective panels. The dashed horizontal lines in the panels indicate the specific receiver offset frequencies $\Delta f = 65$ MHz and $\Delta f = 125$ MHz used in the subsequent examples. To make the OOB interference induced by the transmitter less idealized, moderate intermodulation (resulting from "clipping" of the carrier signal at high amplitudes) was added to the simulation. This results in the intermodulation distortion (IMD) that appears as horizontal bands at frequencies different from the carrier frequency in panels I(a) and II(a).

The upper panels of figure 4 show the instantaneous receiver power averaged over time, for both wide (blue lines) and narrow (red lines) bandwidths of the lowpass filter in the receiver. These would be akin to the power spectra obtained by a spectrum analyzer with the resolution bandwidth (RBW) filters of 5 MHz (red line) and 40 MHz (blue line), without (left panels) and with (right panels) thermal noise taken into account.

Obviously, the *average* receiver power as a function of the RX frequency does not provide information on the peakedness of the receiver signal. The lower panels of figure 4 quantify such peakedness of the receiver signal $z(t) = I(t) + \mathrm{i}Q(t)$ in terms of the measure K_{dBG} found in [8, 11],

$$K_{\mathrm{dBG}}(z) = 10 \lg \left(\frac{\langle |z|^4 \rangle - |\langle zz \rangle|^2}{2\langle |z|^2 \rangle^2} \right), \tag{4}$$

where the angular brackets denote time averaging. This measure of peakedness is based on an extension of the classical definition of *kurtosis* [see 1, for example] to complex variables [see 5, for example]. According to this definition, the peakedness is measured in units of "decibels relative to Gaussian" (dBG) (i.e. in relation to the kurtosis of the Gaussian (aka normal) distribution). Gaussian distribution has zero dBG peakedness, while sub-Gaussian and super-Gaussian distributions have negative and positive dBG peakedness, respectively.

As can be seen in the lower left panel of figure 4, the peakedness of the receiver $I + \mathrm{i}Q$ signal at large values of $|\Delta f|$ is much higher for the wide-bandwidth receiver (blue line) than for the narrow-band receiver (red line). As follows from the linearity property of kurtosis, adding Gaussian (zero dBG) signal to a super-Gaussian (positive dBG) signal would lower the peakedness of the mixture. This can be seen in the lower right panel of figure 4, where the peakedness remains high while the power of the OOB interference dominates over the thermal noise, asymptotically approaching zero as the OOB interference decays at large values of $|\Delta f|$.

Figure 5 provides time (upper panel) and frequency (lower panel) domain quantification of the receiver $I + \mathrm{i}Q$ signal without thermal noise for $\Delta f = 125$ MHz, and wide (blue lines) and narrow (red lines) bandwidths of the lowpass filter.

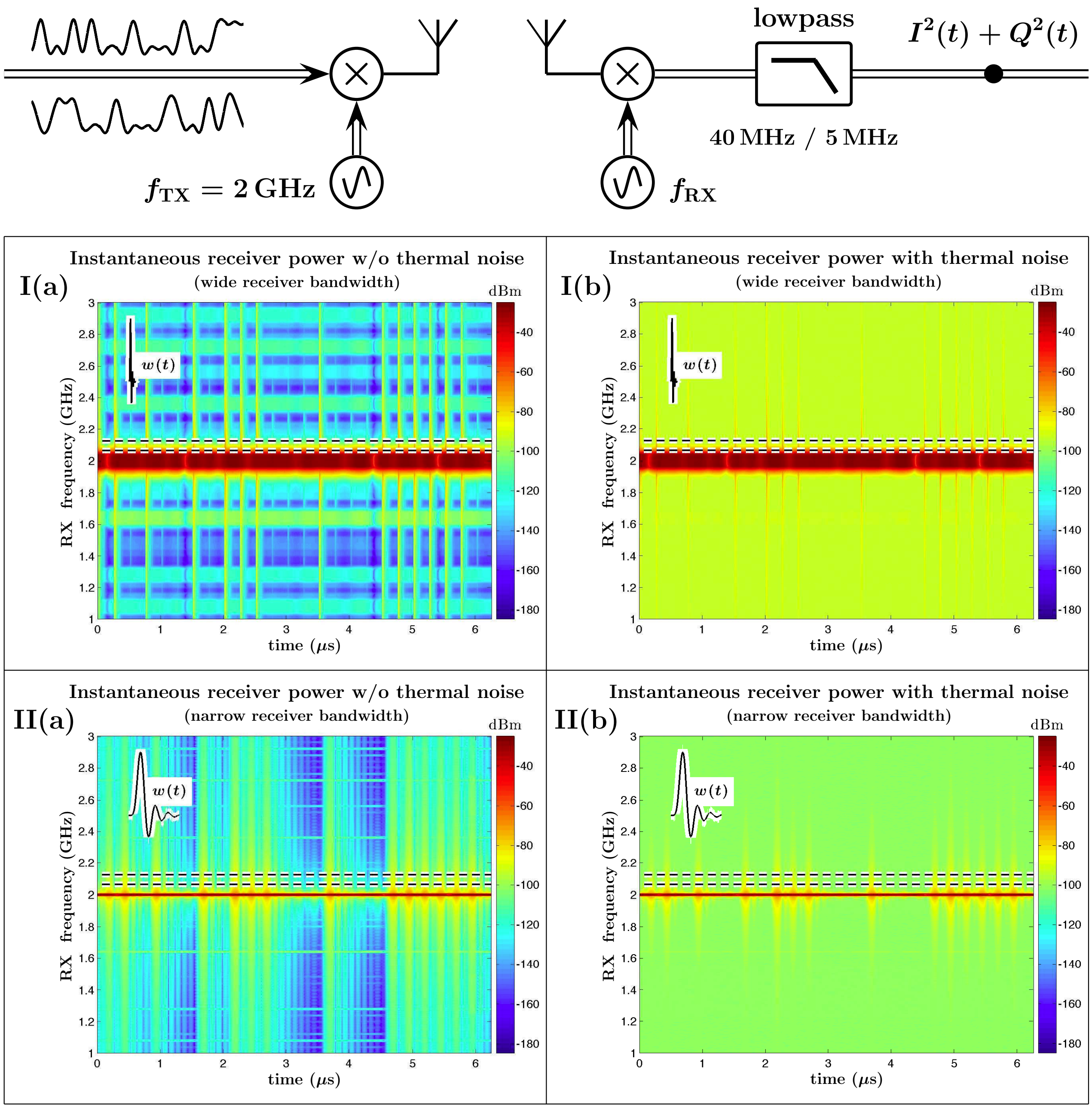

Figure 3: Instantaneous power response of a quadrature receiver tuned to the RX frequency f_{RX} (in the 1 GHz to 3 GHz range). The transmitted signal is in a 5 MHz band around 2 GHz, the transmit power is 125 mW (21 dBm), and the path/coupling loss is 50 dB. *Panels I(a) and I(b):* Wide bandwidth of the lowpass filter (40 MHz 8th order Butterworth filter), without (panel I(a)) and with (panel I(b)) thermal noise. *Panels II(a) and II(b):* Narrow bandwidth of the lowpass filter (5 MHz 8th order Butterworth filter), without (panel II(a)) and with (panel II(b)) thermal noise. The impulse response (time window) $w(t)$ of the lowpass filter is shown in the upper left corners of the respective panels.

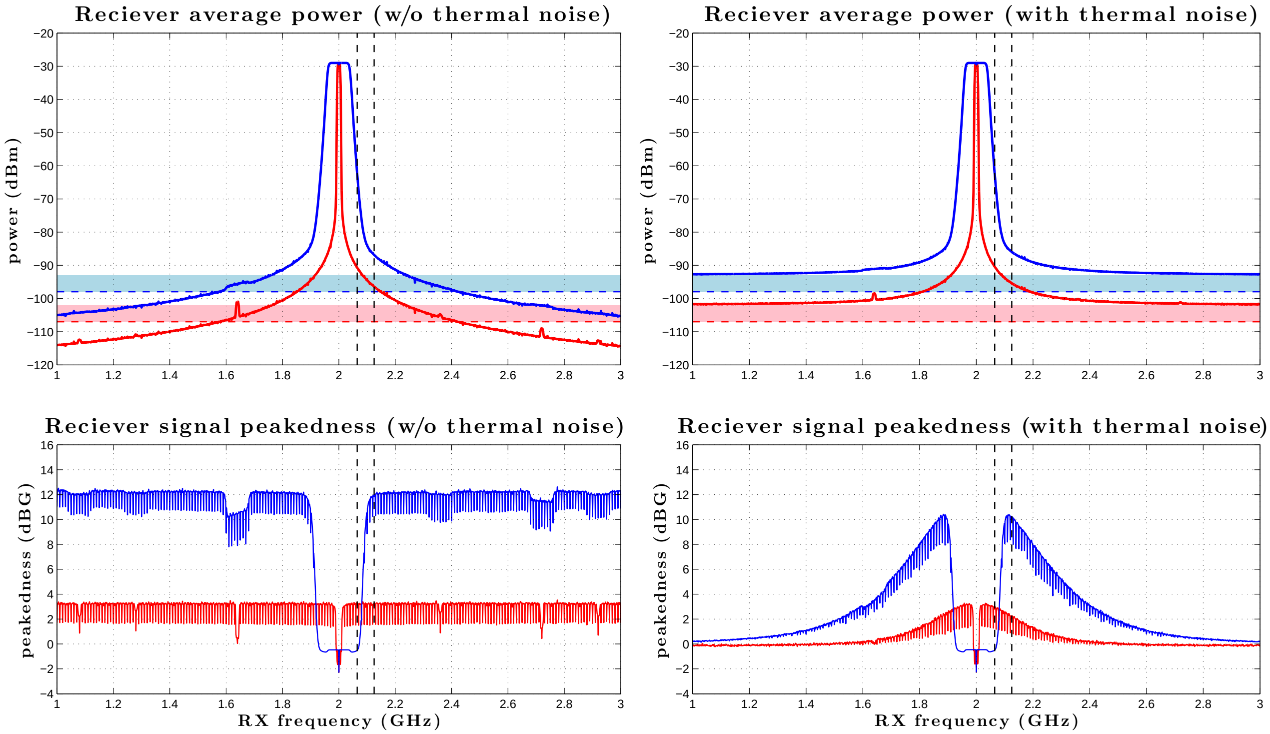

Figure 4: Average power (upper panels) and peakedness (lower panels) of the receiver $I + \mathrm{i}Q$ signal, without (left panels) and with (right panels) thermal noise. The transmitted signal is in a 5 MHz band around 2 GHz, the transmit power is 125 mW (21 dBm), and the path/coupling loss is 50 dB. The receiver lowpass filter is an 8th order Butterworth, with the bandwidth 5 MHz (red lines) and 40 MHz (blue lines). In the upper panels, the thermal noise power is indicated by the horizontal dashed lines, and the width of the shaded bands indicates the receiver noise figure (5 dB).

As additionally discussed in Section 2.1, for a receiver lowpass filter of a given type and order, the amplitude ("height") of the interference pulses would be proportional to the bandwidth of the filter. This can be seen in the upper panel of figure 5, where the peak amplitude of the pulses shown by the blue lines (40 MHz filter) is eight times the peak amplitude of the pulses shown by the red lines (5 MHz filter).

Since the duration of the pulses is inversely proportional to the lowpass filter bandwidth, the time average of the squared amplitudes of the pulses would be proportional to the bandwidth, while the average of the amplitudes raised to the 4th power would be proportional to the bandwidth raised to the 3rd power. As a result, the measure of peakedness given by equation 4 would be approximately proportional to a logarithm of the bandwidth. Thus the increase in the bandwidth of the receiver lowpass filter from 5 MHz to 40 MHz (by 9 dB) would result in a 9 dB increase of peakedness. This is confirmed by the measured values of peakedness indicated in the lower panel of figure 5 for the 5 MHz bandwidth filter (3.2 dBG, red text) and the 40 MHz bandwidth filter (12 dBG, blue text).

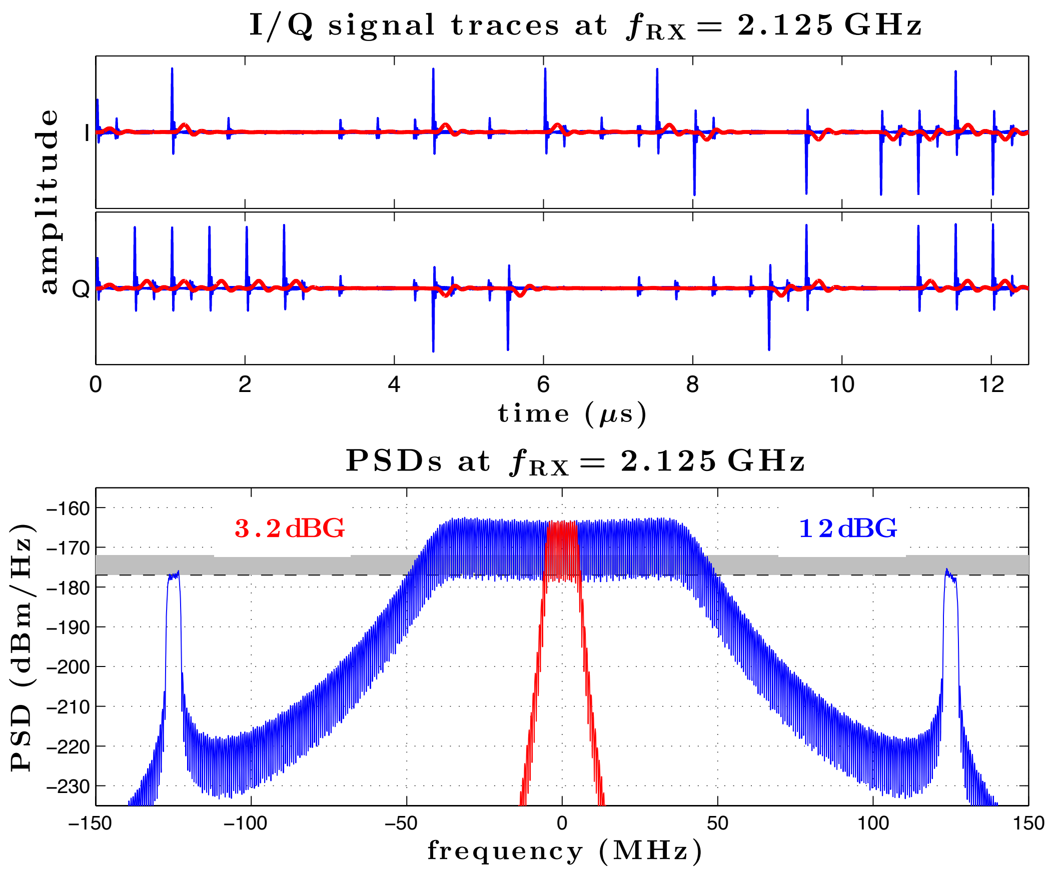

Figure 5: *Upper panel:* In-phase/quadrature (I/Q) signal traces for $f_{\text{RX}} = 2.125\,\text{GHz}$ and the receiver lowpass filters 5 MHz (red lines) and 40 MHz (blue lines). *Lower panel:* Power spectral densities and peakedness of the receiver signal for the receiver lowpass filters 5 MHz (red) and 40 MHz (blue). The thermal noise density is indicated by the horizontal dashed line. The width of the shaded band indicates the receiver noise figure (5 dB).

Not surprisingly, as can be seen in the lower panel of figure 5, the power spectral density (PSD) of the interference around $\Delta f = 0$ (in baseband) is identical for both wide- and narrow-bandwidth receiver filters, and if linear subsequent processing is used (e.g. the signal is digitized and filtered with a matching digital filter), the resulting signal quality is independent of the bandwidth of the lowpass filter in the receiver. However, while the increase in the bandwidth of the receiver lowpass filter does not affect the baseband PSD of either the interference or the thermal noise, widening this bandwidth increases the peakedness of the interference, enabling its more effective mitigation by the Nonlinear Differential Limiters (NDLs) introduced in Section 3.

Figure 6 provides time (upper panel) and frequency (lower panel) domain quantification of the receiver $I + \mathrm{i}Q$ signal without thermal noise for $\Delta f = 65\,\text{MHz}$, for a 40 MHz lowpass filter (green lines), and for a 40 MHz lowpass filter cascaded with a 65 MHz notch filter (black lines).

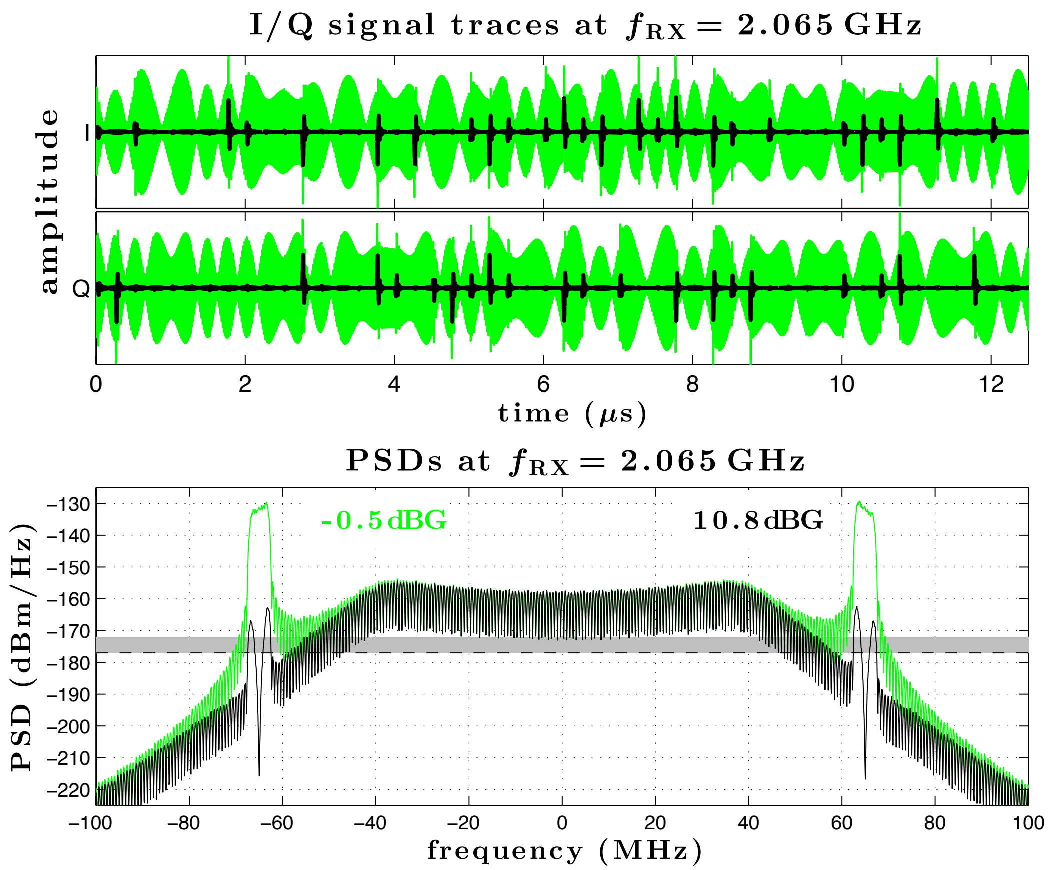

Figure 6: *Upper panel:* In-phase/quadrature (I/Q) signal traces for $f_{RX} = 2.065$ GHz, for a 40 MHz lowpass filter (green lines), and for a 40 MHz lowpass filter cascaded with a 65 MHz notch filter (black lines). *Lower panel:* Power spectral densities and peakedness of the receiver signal for a 40 MHz lowpass filter (green), and for a 40 MHz lowpass filter cascaded with a 65 MHz notch filter (black). The thermal noise density is indicated by the horizontal dashed line. The width of the shaded band indicates the receiver noise figure (5 dB).

The response of the receiver 40 MHz lowpass filter at 65 MHz is relatively large, and, as can be seen in both panels of figure 6 (green lines and text), the contribution of the TX signal in its nominal band (part I of the interference in figure 2) into the total interference becomes significant, reducing the peakedness of the total interference and making it sub-Gaussian (-0.5 dBG peakedness). However, since the sub-Gaussian part of the interference lies outside of the baseband, cascading a 65 MHz notch filter with the lowpass filter would reduce this part of the interference without affecting either the signal of interest or the PSD of the impulsive interference around the baseband. Then, as shown by the black lines and text in figure 6, the interference becomes super-Gaussian (10.8 dBG peakedness), enabling, as illustrated further in Section 4, its effective mitigation by the NDLs introduced in Section 3.

2.1 Effects of symbol rates and pulse shaping on the interference power

When the origins of the OOB interference lie in the finite duration of the finite impulse response (FIR) filters used for pulse shaping, an average value of $t_{i+1} - t_i$ in equation (2) is of the same order of magnitude as the symbol duration (unit interval) T (in the range from $T/2$ to T, and equal to T if the group delay is a multiple of T). If the reciprocal of this value (the symbol rate) is small in comparison with the bandwidth of the receiver, the contribution of the terms $\alpha_i \alpha_j^* h\left(\bar{t} - \bar{t}_i\right) h\left(\bar{t} - \bar{t}_j\right)$ for $i \neq j$ is negligible, and equation (2) describes an impulsive pulse train consisting of a linear combination of pulses shaped as $w^2(t)$ and originating at $\{t_i\}$, namely

$$P_x(t, \Delta f) = \frac{1}{(T\,\Delta f)^{2n}} \sum_i |\alpha_i|^2\, h^2\left(\bar{t} - \bar{t}_i\right) \quad (5)$$

for sufficiently large T and Δf .

In equation 5, the terms under the summation sign are functions of the nondimensionalized time $\bar{t} = \frac{2\pi}{T}\,t$. Then, for a given transmitter power and the modulation pulse shape, if the discontinuities are due to the modulation pulse shape only and thus the time intervals between t_i and t_{i+1} are proportional to the unit interval T, the differences between $\bar{t}_i$ and $\bar{t}_{i+1}$ and thus the time average of the sum in equation 5 are independent of the symbol rate. As a result, provided that the conditions for equation 5 are met, for given offset frequency Δf, transmitter power, and the modulation pulse shape, the average interference power is proportional to the symbol rate raised to the power of $2n$.

This is illustrated in figure 7, where the upper panel shows the (highly oversampled) FIR root-razed-cosine filters [12] used for pulse shaping. All four filters have group delays equal to three times the unit interval T, two with roll-off factor 1/4 (red and blue lines), and two with roll-off factor zero (black and green lines). The non-zero end values of the filters shown by the red and blue lines lead to discontinuities in the modulation signal ($n = 1$). The ratio of the unit intervals for these filters is equal to 2 (for the symbol rates 2 Mbit/s and 1 Mbit/s, respectively), and thus the ratio of the respective interference powers at high Δf is $2^{2n} = 2^2$, or 6 dB, as can be seen in the middle panel of figure 7.

While for the filters shown by the black and green lines the modulating signal itself will be continuous (the end values are zero), the first time derivative of the modulation signal will be discontinuous ($n = 2$). The ratio of the unit intervals for these filters is equal to 4 (for the symbol rates 8 Mbit/s and 2 Mbit/s, respectively), and thus the ratio of the respective interference powers at high Δf is $4^{2n} = 4^4$, or 24 dB, as can be seen in the middle panel of figure 7.

As can be seen in the lower panel of figure 7, as the offset frequency Δf increases, the impulsive component of the OOB interference becomes dominant, leading to a high peakedness of the interference.

As can also be seen from equation 5, the average interference power depends on the impulse response $w(t)$ of the receiver lowpass filter, and, for a filter of a given type and order, is proportional to its bandwidth. On the other hand, the thermal noise power is also proportional to the bandwidth of the receiver lowpass filter, and thus the ratio of the powers of the interference and the thermal noise is independent of this bandwidth. This can be seen in the upper panels of figure 4, where the increase in the bandwidth of the receiver lowpass filter from 5 MHz to 40 MHz (by 9 dB) results in a 9 dB increase of both the interference and the thermal noise powers.

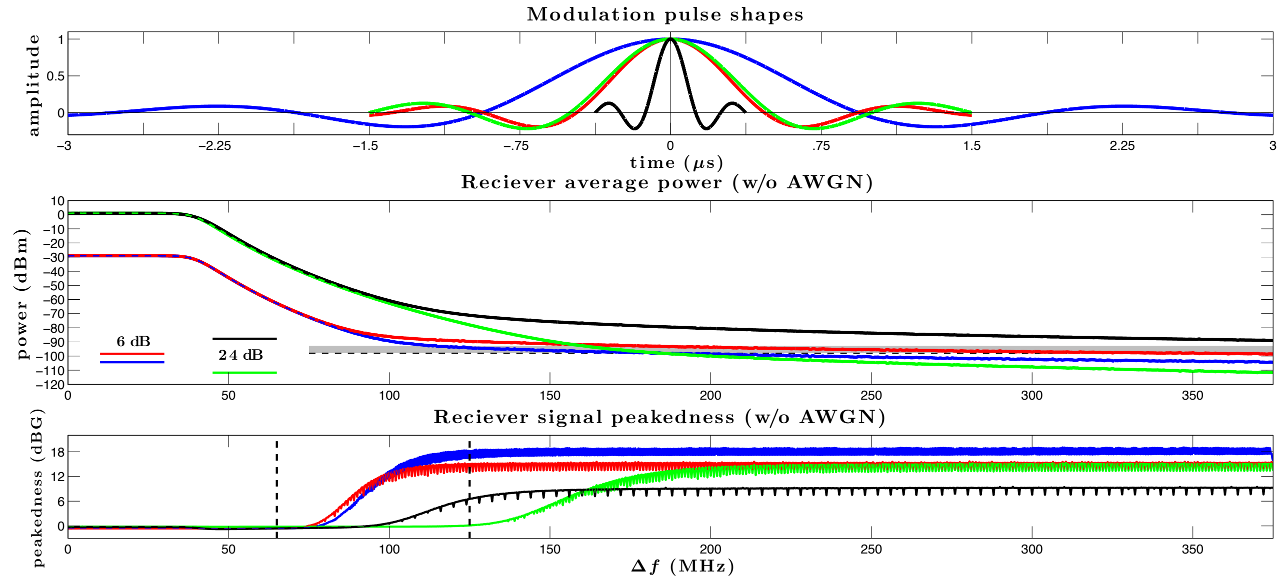

Figure 7: Effects of symbol rates and pulse shaping on the interference power and peakedness.

While the increase in the bandwidth does not affect the baseband PSD of either the interference or the thermal noise, widening of this bandwidth increases the peakedness of the interference, enabling its more effective mitigation by the NDLs introduced in the next section.

3 Nonlinear differential limiters

In this section, we provide a brief introduction to the NDLs. More comprehensive descriptions of the NDLs, with detailed analysis and examples of various NDL configurations, non-adaptive as well as adaptive, can be found in [9, 8, 11].

Let us consider a linear analog filter consisting of cascaded filtering stages and comprising a second order lowpass stage. Such a second order lowpass stage (a lowpass filter) can be described by a differential equation

$$\zeta(t) = z(t) - \tau\,\dot{\zeta}(t) - (\tau Q)^2\,\ddot{\zeta}(t)\,, \tag{6}$$

where $z(t)$ and $\zeta(t)$ are the input and the output signals, respectively (which can be real-, complex-, or vector-valued), τ is the *time parameter* of the stage, Q is the quality factor, and the dot and the double dot denote the first and the second time derivatives, respectively. Note that, when written in such a form, equation (6) with $Q = 0$ describes a first order lowpass filter.

For a linear time-invariant filter the time parameter τ and the quality factor Q in equation (6) are constants, so that when the input signal $z(t)$ is increased by a factor of K, the output $\zeta(t)$ is also increased by the same factor, as is the difference between the input and the output. For convenience, we will call the difference between the input and the output $z(t) - \zeta(t)$ *the difference signal*. A transient outlier in the input signal would result in a transient outlier in the difference signal of a filter, and an increase in the input outlier by a factor of K would result, for a linear filter, in the same factor increase in the respective outlier of the difference signal. If a significant portion of the frequency content of the input outlier is within the passband of the linear filter, the output will typically also contain an outlier corresponding to the input outlier, and the amplitudes of the input and the output outliers will be proportional to each other. A reduction (limiting) of the output outliers, while preserving the relationship between the input and the output for the portions of the signal not containing the outliers, can be achieved by proper dynamic modification of the filter parameters τ and Q in equation (6) based on the magnitude (for example, the absolute value) of the difference signal. A filter comprising such dynamic modification of the filter parameters based on the magnitude of the difference signal will be called a Nonlinear Differential Limiter (NDL).

Since at least one of the filter parameters depends on the instantaneous magnitude of the difference signal, the differential equation describing such a filter is nonlinear. However, even though in general an NDL is a nonlinear filter, if the parameters remain constant as long as the magnitude of the difference signal remains within a certain range, the behavior of the NDL will be linear during that time. Thus an NDL can be configured to behave linearly as long as the input signal does not contain outliers. By specifying a proper dependence of the NDL filter parameters on the difference signal it can be ensured that, when the outliers are encountered, the nonlinear response of the NDL limits the magnitude of the respective outliers in the output signal.

A comprehensive discussion and illustrative examples of various dependencies of the NDL parameters on the difference signal can be found in [9, 8, 11]. For example, one can set the quality factor in equation (6) to a constant value, and allow the time parameter τ be a *non-decreasing* function of the absolute value of the difference signal satisfying the following equation:

$$\tau(|z-\zeta|) = \tau_0 \times \begin{cases} 1 & \text{for} \quad |z-\zeta| \le \alpha \\ >1 & \text{otherwise} \end{cases}, \tag{7}$$

where $\alpha > 0$ is the *resolution* parameter. A particular example can be given by

$$\tau(|z-\zeta|) = \tau_0 \times \begin{cases} 1 & \text{for} \quad |z-\zeta| \le \alpha \\ \left(\frac{|z-\zeta|}{\alpha}\right)^{\beta} & \text{otherwise} \end{cases} \tag{8}$$

with $\beta > 0$, resulting in a Canonical Differential Limiter (CDL) for $\beta = 1$, or a Differential over-Limiter (DoL) for $\beta > 1$.

It should be easily seen from equations (7) or (8) that in the limit of a large resolution parameter, $\alpha \to \infty$, an NDL becomes equivalent to the respective linear filter with $\tau = \tau_0 = \text{const}$. This is an important property of the proposed NDL, enabling its full compatibility with linear systems. At the same time, when the noise affecting the signal of interest contains impulsive outliers, the signal quality (e.g. as characterized by a signal-to-noise ratio (SNR), a throughput capacity of a communication channel, or other measures of signal quality) exhibits a global maximum at a certain finite value of the resolution parameter $\alpha = \alpha_0$, as illustrated in figures 8 and 10 of the next section.

In the limit of a large resolution parameter, an NDL is equivalent to the respective linear filter with $\tau = \tau_0 = \text{const}$, resulting in the same signal quality of the filtered output as provided by the linear filter, whether the noise is a purely AWGN or it contains an impulsive component. When viewed as a function of the resolution parameter, however, when the noise contains an impulsive component the signal quality of the NDL output would exhibit a global maximum. This property of an NDL enables its use for improving the signal quality in excess of that achievable by the respective linear filter, effectively reducing the spectral density of the interference in the signal passband without significantly affecting the signal of interest.

The value of α_0 that maximizes the signal quality may vary in a wide range depending on the composition of the signal+noise mixture, for example, on the SNR and the relative spectral and temporal structures of the signal and the noise. Adaptive NDL (ANDL) configurations (see [9, 8, 11]) contain a sub-circuit (characterized by a *gain* parameter) that monitors a chosen measure of the signal+noise mixture and provides a time-dependent resolution parameter $\alpha = \alpha(t)$ to the main NDL circuit, making it suitable for improving quality of non-stationary signals under time-varying noise conditions.

4 Mitigation of out-of-band interference

As was stated earlier, NDLs can improve the quality of a signal affected by impulsive noise in excess of that achievable by the respective linear filters, increasing the capacity of a communications channel in the presence of such noise. In this section, we provide examples of mitigating the OOB interference discussed in Section 2 by the NDLs.

The incoming "native" (in-band) RX signal used in the examples of figures 8 through 11 was a QPSK signal with the I/Q modulating signals as two independent random bit sequences with the rate 4.8 Mbit/s. An FIR root-raised-cosine (RRC) filter with roll-off factor 1/4 and group delay $3T$ was used for the RX incoming signal pulse shaping, and the same FIR filter was used for matched filtering in the baseband. In all examples, the signal-to-noise ratio for the RX signal was measured in the baseband, after applying the matched FIR filter.

The PSD of the RX signal without noise was approximately -167 dBm/Hz in the baseband, leading to the S/N ratio without interference of approximately 5 dB, as indicated by the upper horizontal dashed lines in figures 8 and 10. The OOB interference was created by the TX signal used in the examples of Section 2. In all examples of this section, the NDLs were 4th order "Butterworth-like" filters constructed as a 2nd order constant-Q CDL with the pole quality factor $Q = 1/\sqrt{2+\sqrt{2}}$ and the initial cutoff frequency $f_0 = 5.25$ MHz, followed by a 2nd order linear lowpass filter with $Q = 1/\sqrt{2-\sqrt{2}}$ and the same cutoff frequency.

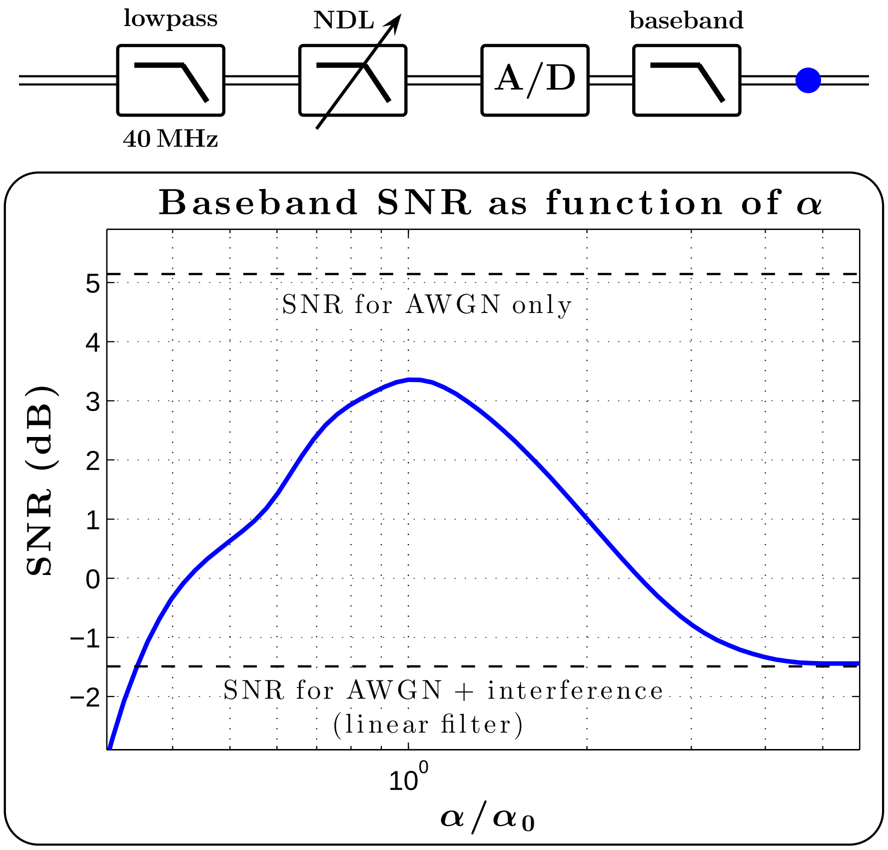

Figure 8: SNR in the receiver baseband as a function of the NDL resolution parameter α. The RX frequency is $f_{\mathrm{RX}} = 2.125$ GHz, and the NDL follows the 40 MHz lowpass filter.

In figures 8 and 9, the receiver with the 40 MHz lowpass filter was tuned to $f_{\mathrm{RX}} = 2.125$ GHz. Figure 8 shows the SNR in the receiver baseband as a function of the NDL resolution parameter α. In the limit of a large resolution parameter, an NDL is equivalent to the respective linear filter (in this example, the 4th order Butterworth lowpass filter with the cutoff frequency $f_0 = 5.25$ MHz), resulting in the same signal quality of the filtered output as provided by the linear filter (indicated by the lower horizontal dashed line). When viewed as a function of the resolution parameter, however, the signal quality of the NDL output exhibits a global maximum at some $\alpha = \alpha_0$. This property of an NDL enables its use for improving the signal quality in excess of that achievable by the respective linear filter, effectively reducing the in-band impulsive interference. As can be seen in figure 8, when linear processing is used, the OOB interference reduces the SNR by approximately 6.7 dB. The NDL with $\alpha = \alpha_0$ improves the SNR by approximately 4.8 dB, suppressing the OOB interference by approximately a factor of 3.

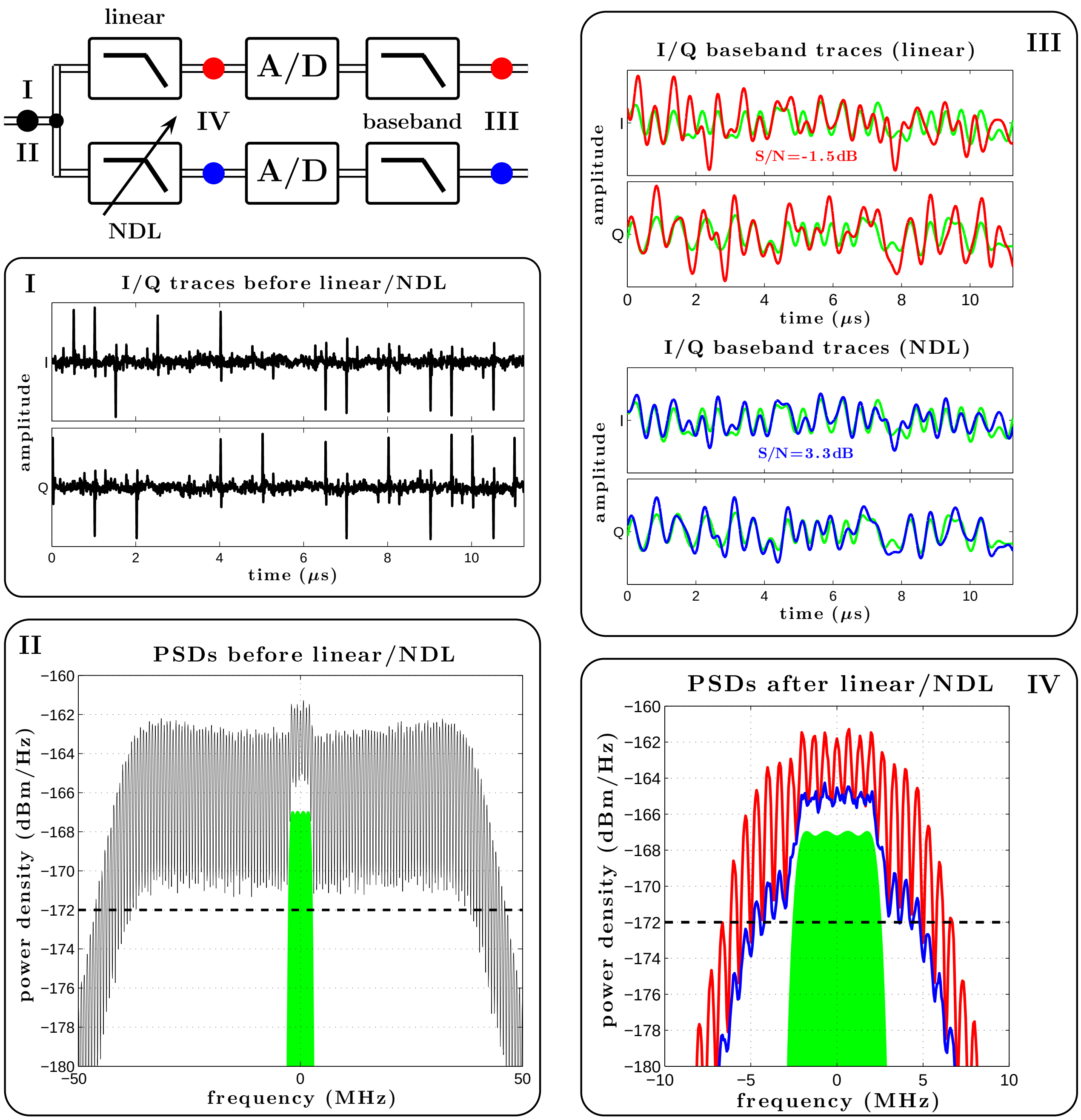

Figure 9: Time domain I/Q traces and PSDs of the signals measured at the test points indicated by the fat colored dots on the signal path diagram in the upper left of the figure. The RX frequency is $f_{\mathrm{RX}} = 2.125\,\mathrm{GHz}$. In panels II and IV, the AWGN level is shown by the horizontal dashed lines, and the PSD of the RX signal without noise is shown by the green shading. In panel III, the green lines show the I/Q traces of the baseband RX signal without noise.

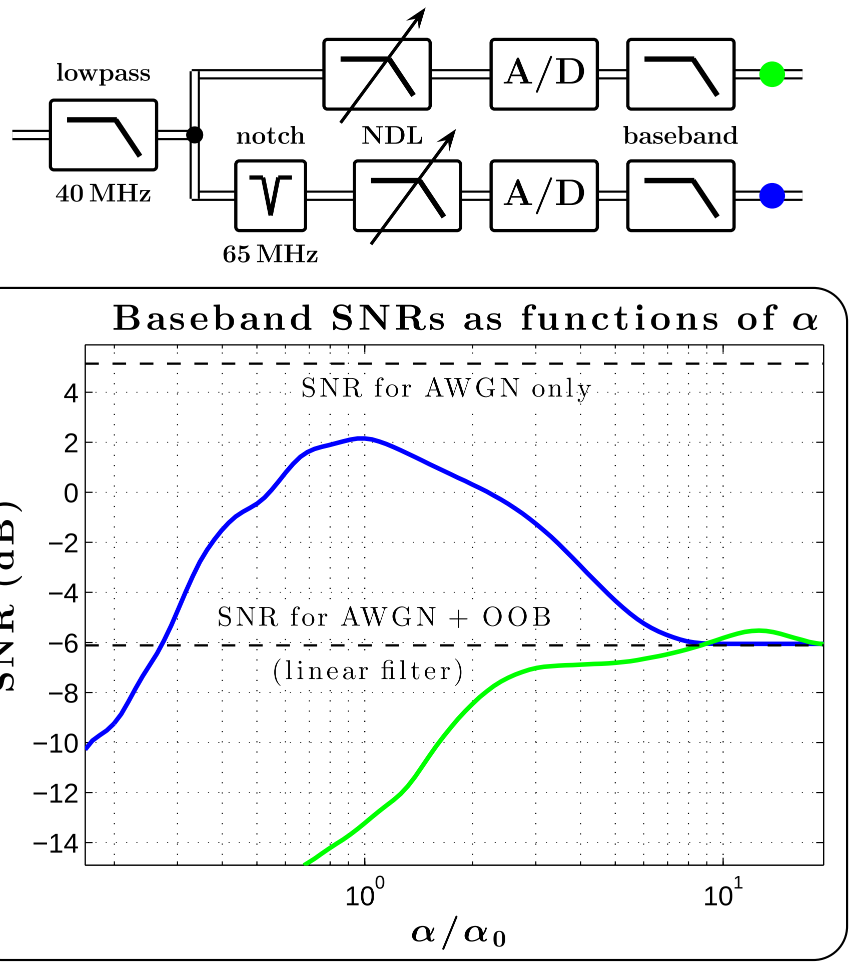

Figure 10: SNRs in the receiver baseband as functions of the NDL resolution parameter α. The RX frequency is $f_{\mathrm{RX}} = 2.065\,\mathrm{GHz}$. *Green line:* The NDL is applied directly to the output of the 40 MHz lowpass filter. *Blue line:* A 65 MHz notch filter precedes the NDL.

For the resolution parameter of the NDL set to $\alpha = \alpha_0$, figure 9 shows the time domain I/Q traces and PSDs of the signals measured at the test points indicated by the fat colored dots on the signal path diagram outlined in the upper left of the figure. In panels II and IV, the AWGN level is shown by the horizontal dashed lines, and the PSD of the RX signal without noise is shown by the green shading. In panel III, the green lines show the I/Q traces of the baseband RX signal without noise. In panel IV of figure 9, the fact that the NDL indeed reduces the spectral density of the interference without significantly affecting the signal of interest can be deduced and gauged from observing how the quasiperiodic structure of the PSD is affected by the NDL in comparison with the linear filter.

If the Shannon formula [13] is used to calculate the capacity of a communication channel, the baseband SNR increase from -1.5 dB to 3.3 dB provided by the NDL in the examples of figures 8 and 9 results in a 114% (2.14 times) increase in the channel capacity.

Figure 10 shows the SNRs in the receiver baseband as functions of the NDL resolution parameter α for the RX frequency $f_{\mathrm{RX}} = 2.065\,\mathrm{GHz}$, when the NDL is applied directly to the output of the 40 MHz lowpass filter (green line), and when a 65 MHz notch filter precedes the NDL (blue line). As can be seen in figure 10 from the distance between the horizontal dashed lines, when linear processing is used, the OOB interference reduces the SNR by approximately 11 dB.

As was discussed in Section 2 (see, in particular, the description of figure 6), the response of the receiver 40 MHz lowpass filter at 65 MHz is relatively large, and the contribution of the TX signal in its nominal band (part I of the interference in figure 2) into the total interference is significant, which makes the total interference sub-Gaussian (-0.5 dBG peakedness). Thus an NDL deployed immediately after the 40 MHz lowpass filter will not be effective in suppressing the interference, as can be seen from the SNR curve shown by the green line in figure 10. However, a 65 MHz notch filter preceding the NDL attenuates the non-impulsive part of the interference without affecting either the signal of interest or the PSD of the impulsive interference, making the interference impulsive and enabling its effective mitigation by the subsequent NDL. This can be seen from the SNR curve shown by the blue line in figure 10, where the NDL with $\alpha = \alpha_0$ improves the SNR by approximately 8.2 dB, suppressing the OOB interference by approximately a factor of 6.6.

For the resolution parameter of the NDL set to $\alpha = \alpha_0$, figure 11 shows the time domain I/Q traces and the PSDs of the signals measured at the test points indicated by the fat colored dots on the signal path diagram in the upper left of the figure. The RX frequency is $f_{\mathrm{RX}} = 2.065\,\mathrm{GHz}$, and the notch is at 65 MHz. In panels II and IV, the AWGN level is shown by the horizontal dashed lines, and the PSD of the RX signal without noise is shown by the green shading. In panel III, the green lines show the I/Q traces of the baseband RX signal without noise. In panel IV of figure 11, the fact that the NDL indeed reduces the spectral density of the interference without significantly affecting the signal of interest can be deduced and gauged from observing how the quasiperiodic structure of the PSD is affected by the NDL in comparison with the linear filter.

If the Shannon formula [13] is used to calculate the capacity of a communication channel, the baseband SNR increase from -6 dB to 2.2 dB provided by the NDL in the examples of figures 10 and 11 results in a 337% (4.37 times) increase in the channel capacity.

5 Concluding remarks

Interference from various technogenic (man-made) sources, unintentional as well as intentional, would typically have temporal and/or amplitude structure, and its amplitude distribution would usually be non-Gaussian. A simplified explanation of non-Gaussian (and often impulsive) nature of a technogenic noise produced by digital electronics and communication systems can be as follows. An idealized discrete-level (digital) signal can be viewed as a linear combination of Heaviside unit step functions [see 2, for example]. Since the derivative of the Heaviside unit step function is the Dirac δ-function [see 4, for example], the derivative of an idealized digital signal is a linear combination of Dirac δ-functions, which is a limitlessly impulsive signal with zero interquartile range and infinite peakedness. The derivative of a "real" (i.e. no longer idealized) digital signal can thus be viewed as a convolution of a linear combination of Dirac δ-functions with a continuous kernel. If the kernel is sufficiently narrow (for example, the bandwidth is sufficiently large), the resulting signal will appear as an impulse train protruding from a continuous background signal. Thus impulsive interference occurs "naturally" in digital electronics as "$\mathrm{d}i/\mathrm{d}t$" (inductive) noise or as the result of coupling (for example, capacitive) between various circuit components and traces, leading to the so-called "platform noise" [see 14, for example].

In this paper, we focus (in Section 2) on a particular illustrative mechanisms of impulsive interference in digital communication systems resulting from the non-smooth nature of any physically realizable modulation scheme for transmission of a digital (discontinuous) message. Even modulation schemes designed to be "smooth," e.g., continuous-phase modulation, are, in fact, not smooth because their higher order time derivatives still contain discontinuities.

The non-Gaussian nature of technogenic interference provides an opportunity for its mitigation by nonlinear filtering that is more effective than the mitigation achievable by linear filters. When a linear filter is used to suppress interference outside the passband of interest, the filtered signal quality is not influenced by the type of the amplitude distribution of the interfering signal, as long as the total power and the spectral composition of the interference is the same. It may be possible to reduce the spectral density of the *in-band* technogenic interference (that is, in the signal's passband) without significantly affecting the signal of interest by introducing an appropriately chosen feedback-based nonlinearity into the response of a filter. As a result, the signal quality can be improved in excess of that achievable by the respective linear filter.

In this paper, we describe (in Section 3) such nonlinear filters, Nonlinear Differential Limiters (NDLs), outline a methodology for mitigation of technogenic interference in communication channels by NDLs, and provide several examples (in Section 4) of such mitigation for the interference produced according to the mechanism outlined in Section 2. We demonstrate that an NDL replacing a linear filter in the receiver channel can improve the receiver by increasing the signal quality in the presence of man-made noise, and thus the capacity of a communication channel.

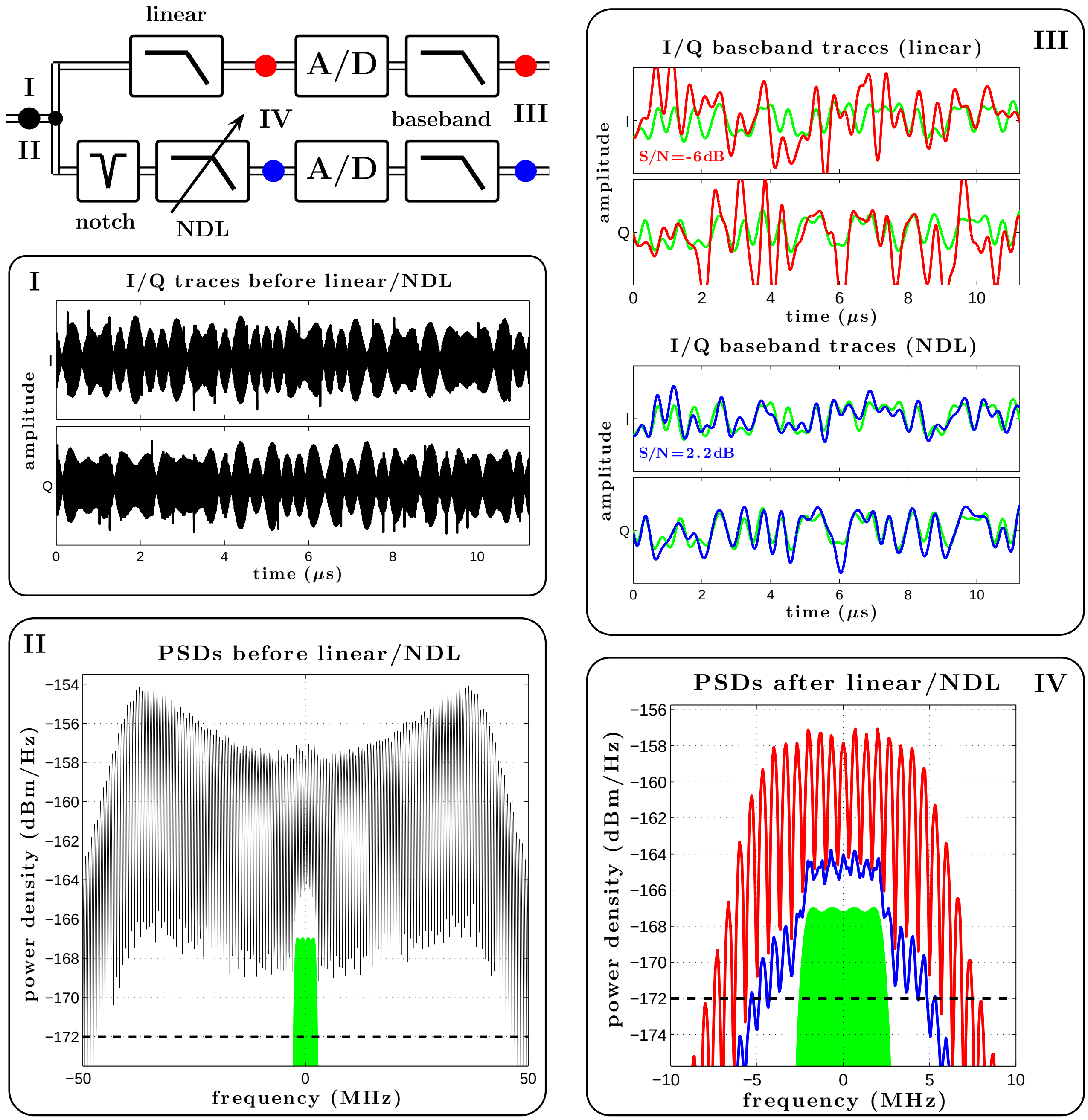

Figure 11: Time domain I/Q traces and PSDs of the signals measured at the test points indicated by the fat colored dots on the signal path diagram in the upper left of the figure. The RX frequency is $f_{\rm RX} = 2.065\,\text{GHz}$, and the notch is at 65 MHz. In panels II and IV, the AWGN level is shown by the horizontal dashed lines, and the PSD of the RX signal without noise is shown by the green shading. In panel III, the green lines show the I/Q traces of the baseband RX signal without noise.

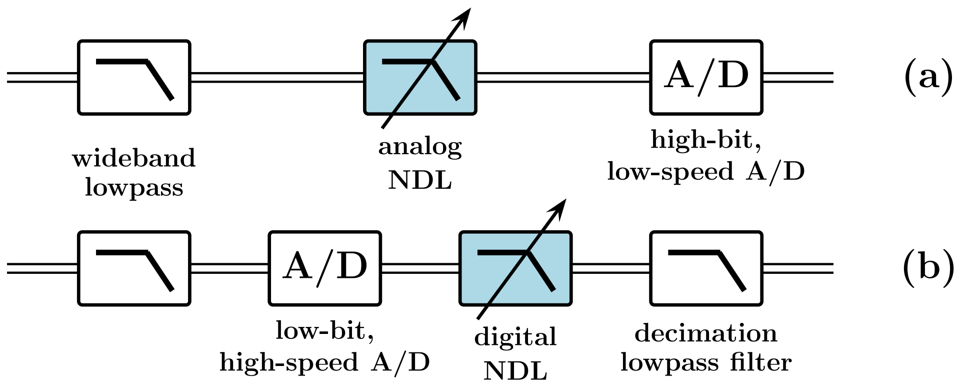

Figure 12: Analog (panel (a)) and digital (panel (b)) NDL deployment.

5.1 Comment on digital NDLs

For the interference to appear strongly impulsive, the bandwidth of the receiver lowpass filter needs to be much larger than a typical value of $(t_{i+1} - t_i)^{-1}$ in equation (2), and effective use of an NDL may require that its input signal has a bandwidth much larger than the bandwidth of the RX signal of interest. Thus the best conceptual placement for an NDL is in the analog part of the signal chain, for example, as part of the antialiasing filter preceding the analog-to-digital converter (ADC), as shown in panel (a) of figure 12. However, digital NDL implementations may offer many advantages typically associated with digital processing, including simplified development and testing, configurability, and reproducibility.

While near-real-time finite-difference implementations of the NDLs described in Section 3 would be relatively simple and computationally inexpensive, their use would still require a digital signal with a sampling rate much higher than the Nyquist rate of the signal of interest. Increasing the sampling rate of a high-resolution converter in order to enable the use of an NDL would be impractical for many reasons, including the ADC cost and its saturation by high-amplitude impulsive outliers. Instead, as illustrated in panel (b) of figure 12, a low-bit high-rate A/D converter should be used to provide the input to a digital NDL. Then the NDL output can be downsampled (after appropriate digital lowpass filtering) to provide the desired high-resolution signal at lower sampling rate.

A Simulation parameters

The transmitter signal used in all simulations was a QPSK signal with the I/Q modulating signals as two independent random bit sequences. In all simulations except those shown in figure 7 the symbol rate was 4 Mbit/s (unit interval $T = 250$ ns), and an FIR RRC filter [see 12, for example] with the roll-off factor 1/4 and the group delay $3T$ was used for pulse shaping. The average TX signal power in all simulations was set to 125 mW (21 dBm), and it was assumed that the additional path/coupling loss at any RX frequency was 50 dB, except for the TX signals shaped with the filters shown by black and green lines in figure 7, where it was 20 dB.

A rather small transmission power (6 dB below a typical cellular phone power of 27 dBm), and relatively large 50 dB loss were chosen as somewhat of a “safety margin" to ensure that, even if the OOB emissions are significantly (e.g. by 20-30 dB) reduced by a carefully selected combination of the roll-off factor and the group delay of the shaping filter, and/or by reducing the bandwidth (symbol rate) of the TX signal, the spectral density of the interference may still be comparable with or dominate over the spectral density of the thermal noise for a respectively smaller path/coupling loss and/or larger transmit power.

The quasiperiodic time domain structures of the spectrograms in figure 3, and of the time domain traces seen in the upper panels of figures 5 and 6, and in panel I of figure 9, are related to the unit interval T and have a period $T = 250\,\mathrm{ns}$. The quasiperiodic structures that can be seen in the PSDs shown in the lower panels of figures 5 and 6, and in panels II and IV of figures 9 and 11, are related to the group delay of the FIR pulse shaping filters, and have a period equal to half of the inverse group delay, or $(6T)^{-1} = 2/3\,\mathrm{MHz}$.

As can be seen in the lower panels of figure 4, the peakedness of the interference also exhibits a quasiperiodic structure (quasiperiodic local minima). This period is related to the symbol rate T^{-1} as $(2\,T)^{-1} = 2\,\mathrm{MHz}$, or half of the symbol rate. In those simulations, the f_{RX} sampling interval of 1.25 MHz was used. This is why only one out of four local minima are visible, and the apparent period of peakedness in figure 4 is 10 MHz. The local minima in the peakedness plots shown in the lower panel of figure 7 also occur at halves of the respective symbol rates. For example, the peakedness shown by the black line has a structure with the period 4 MHz.

A constant 5 dB noise figure of the receiver was assumed at all receiver frequencies f_{RX}. This, combined with the -177 dBm/Hz two-sided PSD of the thermal noise at room temperature, leads to the total AWGN noise level of -172 dBm/Hz. The incoming RX signal used in figures 8 through 11 was a QPSK signal with the I/Q modulating signals as two independent random bit sequences with the rate 4.8 Mbit/s. An FIR RRC filter with roll-off factor 1/4 and group delay $3T$ was used for the RX incoming signal pulse shaping, and the same FRI filter was used for the matched filtering in the baseband. The PSD of the RX signal without noise was approximately -167 dBm/Hz in the baseband, leading to the S/N ratio without interference of approximately 5 dB.

B Abbreviations

ACI: Adjacent-Channel Interference; A/D: Analog-to-Digital; ADC: Analog-to-Digital Converter; AMC: Adaptive Modulation and Coding; ANDL: Adaptive Nonlinear Differential Limiter; AWGN: Additive White Gaussian Noise; dBm: dB per milliwatt; DoL: Differential over-Limiter; EMC: Electromagnetic Compatibility; EMI: Electromagnetic Interference; FIR: Finite Impulse Response; IMD: Intermodulation distortion; I/Q: Inphase/Quadrature; MANET: Mobile Ad Hoc Network; Mbit/s: megabit per second; NDL: Nonlinear Differential Limiter; OOB: Out-Of-Band; PSD: Power Spectral Density; QAM: Quadrature Amplitude Modulation; QPSK: Quadrature Phase-Shift Keying (4-QAM); RBW: Resolution Bandwidth (electronic signal term used in spectrum analyzers and EMI/EMC testing); RF: Radio Frequency; RRC: Root Raised Cosine; RX: Receiver; SDR: Software Defined Radio; S/N: Signal-to-Noise; SNR: Signal to Noise Ratio; TX: Transmitter.

References

[1] Abramowitz, M. & Stegun, I. A. , editors. 1972 *Handbook of Mathematical Functions with Formulas, Graphs, and Mathematical Tables*. 9th printing. New York: Dover.

[2] Bracewell, R. 2000 *The Fourier Transform and Its Applications*, chapter "Heaviside's Unit Step Function, $H(x)$", pages 61–65. McGraw-Hill, New York, 3rd edition.

[3] Cohen, L. 1995 *Time-frequency analysis*. Prentice-Hall, Englewood, NJ.

[4] Dirac, P. A. M. 1958 *The Principles of Quantum Mechanics*. Oxford University Press, London, 4th edition.

[5] Hyvärinen, A., Karhunen, J. & Oja, E. 2001 *Independent component analysis*. Wiley, New York.

[6] Nikitin, A. V. 2011 On the impulsive nature of interchannel interference in digital communication systems. In *Proc. IEEE Radio and Wireless Symposium*, pages 118–121, Phoenix, AZ.

[7] Nikitin, A. V. 2011 On the interchannel interference in digital communication systems, its impulsive nature, and its mitigation. *EURASIP Journal on Advances in Signal Processing*, 2011(137).

[8] Nikitin, A. V. 2013 Method and apparatus for signal filtering and for improving properties of electronic devices. US Patent Application Publication 2013/0339418, Dec. 19.

[9] Nikitin, A. V. 2013 Method and apparatus for signal filtering and for improving properties of electronic devices. US patent 8,489,666, July 16.

[10] Nikitin, A. V., Epard, M., Lancaster, J. B., Lutes, R. L. & Shumaker, E. A. 2012 Impulsive interference in communication channels and its mitigation by SPART and other nonlinear filters. *EURASIP Journal on Advances in Signal Processing*, 2012(79).

[11] Nikitin, A. V., Davidchack, R. L. & Sobering, T. J. 2013 Adaptive analog nonlinear algorithms and circuits for improving signal quality in the presence of technogenic interference. In: *Proceedings of IEEE Military Communications Conference 2013 (MILCOM 2013)*, San Diego, CA, Nov. 18-20.

[12] Proakis, J. G. & Manolakis, D. G. 2006 *Digital signal processing: principles, algorithms, and applications*. Prentice Hall, 4th edition.

[13] Shannon, C. E. 1949 Communication in the presence of noise. *Proc. Institute of Radio Engineers*, 37(1):10–21, Jan.

[14] Slattery, K. & Skinner, H. 2008 *Platform Interference in Wireless Systems*. Elsevier.

